MRS Communications (2024) 14:167–177

https://doi.org/10.1557/s43579-024-00538-3

MRS Communications

Organic and Perovskite Materials and Devices Prospective

Recent advancements in achieving high dielectric constant polymer dielectrics for low-power-consumption organic field-effect transistors

Yang Li, Mingqian He, Organic & Biochemical Technologies, Corning Research & Development Corporation, Corning, NY 14831, USA

Address all correspondence to Yang Li at **liy15@corning.com**

(Received 19 September 2023; accepted 4 March 2024; published online: 18 March 2024)

Abstract

While efforts have been made to optimize organic semiconducting materials to achieve low-power-consumption organic field-effect transistors (OFETs), it is important to note that the choice of gate dielectric materials is equally critical. In general, a high-*k* polymer dielectric material is highly preferred for low-power-consumption OFETs. In this perspective, we highlight several newly emerged strategies for high dielectric constant polymer dielectrics. By exploiting the recent advances in molecular modulation and morphology control, these new strategies enable remarkably high dielectric constant up to 25–30 for polymer dielectrics, while still maintaining dielectric losses below 0.01 at 1 kHz. We further analyze the advantages and disadvantages of these strategies and propose four design principles—side-chain dipole, rigid free volume, self-assembly, and thermosets—for future polymer gate dielectrics in OFETs.

Introduction

Since the fabrication of the first polythiophene organic field-effect transistor (OFET) in 1986,[1] research on OFETs has made significant progress over the last 37 years. Starting from the 2010s, OFET-based devices have demonstrated great performances in soft electronics[2–4] and chemical sensors,[5] better exploiting the intrinsic advantages of OFETs over inorganic transistors in terms of mechanical flexibility, low-temperature solution processibility, biocompatibility, and chemical sensitivity/selectivity. To date, with the field-effect mobility of OFET far exceeding 1 $cm^2\ V^{-1}\ s^{-1}$, researchers have increasingly shifted their focus from single OFET device fabrication to large-scale organic circuits integration and product miniaturization, laying the foundations for future industrial applications such as electronic skins,[6,7] bio-sensors,[8–12] and robotics in the era of IoT and artificial intelligence. Accordingly, low-power-consumption OFETs[13] are highly desired because most of the abovementioned applications are portable devices driven by low-voltage batteries.

While enormous efforts have been dedicated to organic semiconducting materials to achieve low-power-consumption OFETs, it should be noted that the choice of gate dielectric materials is equally crucial. Critical OFET performances such as operational voltage, threshold voltage, charge mobility, gate leakage current, and off-state current heavily depend on the attributes of gate dielectric materials, with high dielectric constant (high-*k*) and low loss being the most desired,[14–17] as high-*k* leads to low operational voltage, while low loss means less heat generated during device operating. In general, polymer gate dielectrics[18] are preferred over its inorganic[19,20] and hybrid[21,22] counterparts for OFET-based devices due to better material and processing compatibility than inorganic dielectrics, and superior material homogeneity and dielectric loss compared to hybrid dielectrics. As Zhu mentioned in his high-cited perspective article,[23] among the three main polarization mechanisms that can substantially enhance dielectric constant, e.g., dipolar, ionic, and interfacial polarization, dipolar polarization is the preferred strategy for polymer dielectrics, as it in most cases maintains lower dielectric losses than the other two mechanisms. Furthermore, he proposed that enhancing dipole mobility could substantially increase dipole mobility.

In the following sections, after a brief review of traditional high-polar polymer dielectrics [Fig. 1(a), (b)], we selectively highlight several newly emerged strategies for high-*k* polymer dielectrics in the past 5 years [Fig. 1(c)–(f)]. By providing a personal perspective on the advantages and disadvantages of these strategies, we intend to assist the organoelectronic community in designing and selecting polymer gate dielectric materials for future low-power-consumption OFETs.

Traditional high-polar polymer dielectrics

Main-chain polymer dielectrics

For main-chain polymer dielectrics, increasing interchain distances is an effective way for improving dipole mobility. For example, Xu and coworkers reported a series of aromatic carbonyl-containing polyimides,[24] among which the one with carbonyl moiety in dianhydride and sulfonyl moiety in diamine exhibited the best dielectric performance. The authors attributed the increased dielectric constant (5.23, 1 kHz) and very low loss (0.00324, 1 kHz) to friction-free dipole rotation facilitated by enlarged inter-molecular *d*-spacing.[25]

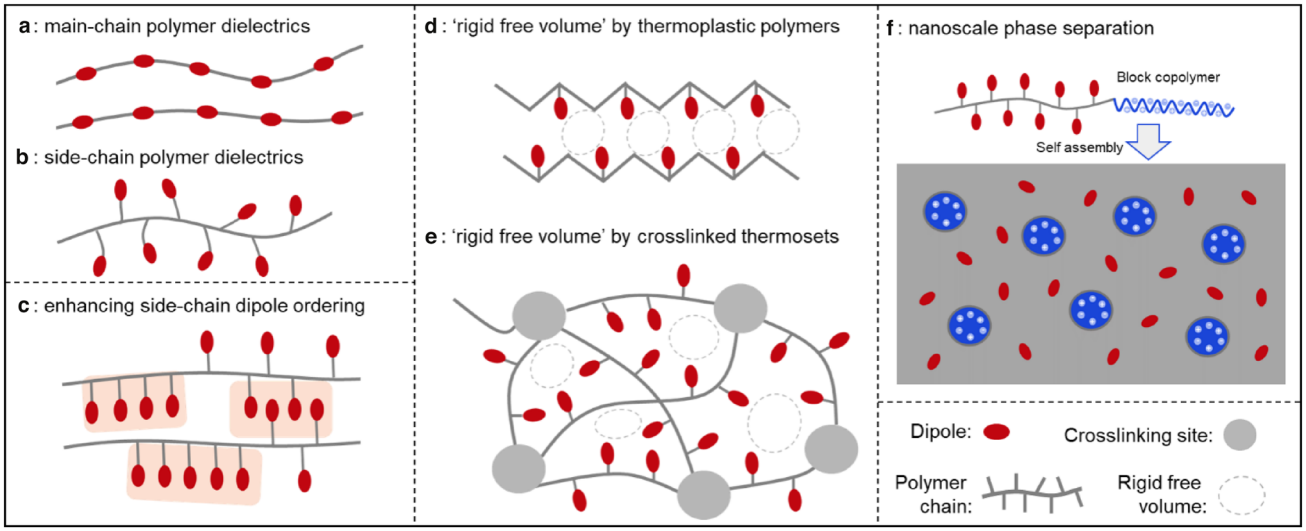

Figure 1. Schematics representing traditional (a, b) and newly emerged strategies (c–f) for high-*k* polymer dielectrics.

Another way to create interchain spacing is blending. By simply mixing an poly(arylene ether urea) (PEEU, k=4.7), and an aromatic polythiourea (ArPTU, k=4.4), Zhang and coworkers made a series of polymer blends featuring much higher dielectric constant up to 8.6 (1 kHz).[28] The significant dielectric constant increase was attributed to an increased interchain spacing in blends' amorphous domains, which effectively reduced the steric barriers for dipole reorientation. The same principle was also applied by Li and Yang,[26] who reported that higher quenching temperatures led to enlarged interdomain spacing of the alicyclic polythiourea APTU-1 [Fig. 2(a)], resulting in remarkable dielectric constant improvement from ~5 to ~9 (1 kHz).

A more sophisticated study from Kong and Cai demonstrated that introducing a polar group Biuret of high dipole moment (4.96 D) into the backbone of PA11 not only significantly improved dipole density of the new Nylon (COPAs), but also increased interchain distances and created large amount of weakly hydrogen-bonded dipoles that are more susceptible to reorientation under external electric field [Fig. 2(b)].[27] As a result, COPAs showed prominent

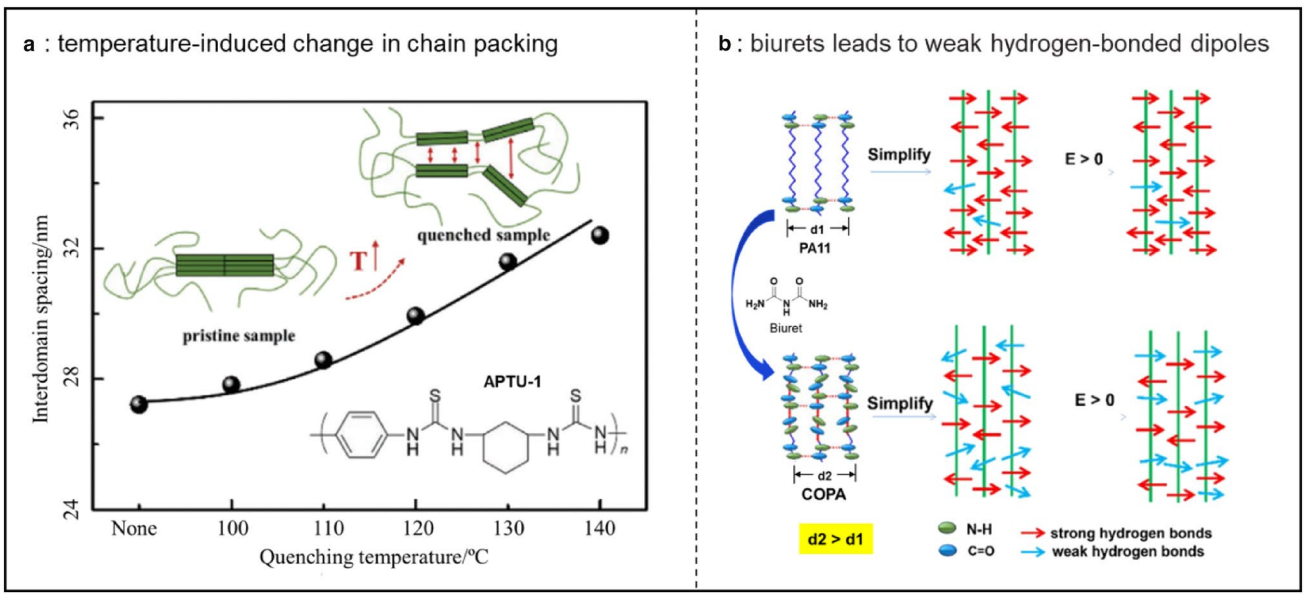

Figure 2. (a) The schematic diagram of the temperature-induced change in the chain packing, the green square represents the ordered structure.[26] Copyright 2020 WILEY–VCH Verlag GmbH & Co. KGaA, Weinheim. (b) Strong hydrogen bonds result in difficult dipole orientation of PA11 (above); introducing biuret segments leads to weak hydrogen-bonded dipoles of COPA that are more susceptible to reorientation (below).[27] Copyright 2022 The Polymer Society, Taipei.

dielectric constant improvement from 5.7 to 10.8 (20 °C, 10 Hz), with only minor increase in dielectric loss.

Main-chain polymer dielectrics, such as high-polar polyimides, have been intensively investigated as high-temperature energy storage materials due to their high thermal stability and high breakdown strength (E_b).[29,30] However, traditional high-polar main-chain polymer dielectrics are limited in achieving high dielectric constant, typically below 10. Additionally, their poor solubilities in commonly used organic solvents make it challenging to process them with solution-based techniques that are generally required for OFET fabrication, such as spin coating.

Side-chain polymer dielectrics

In recent years, the sulfonyl group has garnered significant attention. Apart from its notably high dipole moment (4.25 D vs. 3.9 D for CN), sulfonyl also exhibits minimal space required for rotation (32.3 Å^3 vs. 34.7 Å^3 for –CH_2CN). In 2014, Zhu and coworkers introduced sulfonyl as a side-chain dipole in an acrylic polymer PMSEMA [Fig. 3(a)].[31] The resulting polymer displayed a substantially improved dielectric constant of 10.5 at 1 kHz, coupled with relatively low loss (~0.02). These enhancements were primarily attributed to a notably high percentage of dipole rotation (37–39%), facilitated by the strong γ relaxation at temperatures as low as −110°C.

To enhance dielectric properties at high temperature, Zhu and coworkers synthesized sulfonylated PPO SO_2–PPO_{25} and SO_2–PPO_{52} with relatively high dielectric constants of 5.9 and 8.2 (rt, 1 kHz), respectively.[32] The significantly lower dielectric loss (0.003) compared to PMSEMA was primarily attributed to the rigid amorphous backbone and higher T_g (250°C) of SO_2–PPO. The concept of combining a high T_g backbone with a flexible side-chain dipole was further extended to sulfonylated poly (ether ether ketone)[33] and polyimides.[34] However, it is important to note that simply increasing side-chain dipole density does not necessarily enhance the dielectric constant proportionally. In fact, the increase in dipole density can strengthen dipole–dipole interactions and steric hindrances, leading to reduced average dipole mobility [Fig. 3(b)].[35]

In addition to sulfonyl, various other dipoles such as cyanate,[36] cyclic carbonate,[37] carboxyl,[38] glycidyl,[39] and sulfonic acid,[40] among others, have been reported for side-chain polymer dielectrics. Side-chain polymer dielectrics are more promising in achieving high dielectric constant compared to its main-chain counterparts, as the side-chain dipole rotation can occur via sub-T_g transitions at much lower temperatures, i.e., between β relaxation and T_g, or even between γ and β relaxations. Moreover, side-chain polymer dielectrics are more compatible with solution-based coating techniques. As a result, they are frequently utilized as gate dielectrics for OFETs.

New strategies

Enhancing side-chain dipole ordering

Side-chain dipole self-assembly

In 2013, Tang and coworkers reported very high dielectric constants (11.4–10.2 from 100 Hz to 4 MHz) for a methacrylic polymer with oligothiophene side chain. The greatly improved and almost constant dielectric constant over wide range of frequencies was ascribed to additional electronic and interfacial polarizations facilitated by the self-assembled oligothiophene nano-crystalline domains [Fig. 4(a)].[41] In this case, the very-well dispersed conductive nano-crystalline domains (<2 nm) were covalently bonded to the insulating polymer backbone, creating homogeneous yet still well-defined interfaces that not only enabled interfacial polarization, but also prevented high dielectric loss. In contrast, polynorbornenes containing side-chain oligothiophenes were amorphous polymers without any nano-crystalline domains, which is probably due to the increased distances between the side-chain oligothiophenes.[42] Therefore, the dielectric constant was reduced dramatically to around 4. In another study, the π–π stacking among side-chain biphenyls were harnessed to improve the ordering of side-chain

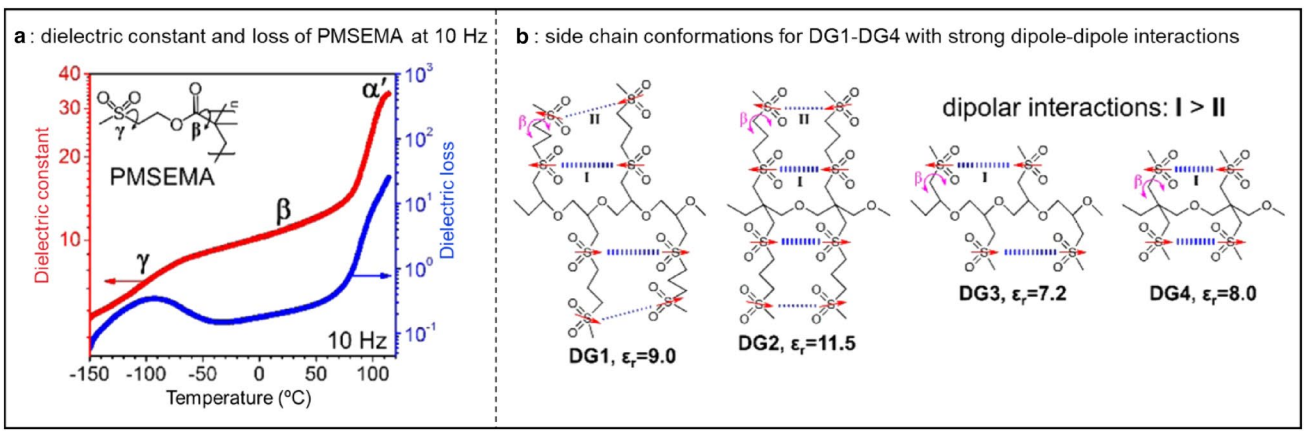

Figure 3. (a) Molecular structure of PMSEMA and its dielectric constant and loss at 10 Hz.[31] Copyright 2015 American Chemical Society. (b) Proposed side-chain conformations for DG1–4 with strong dipole–dipole interactions.[35] Copyright 2018 American Chemical Society.

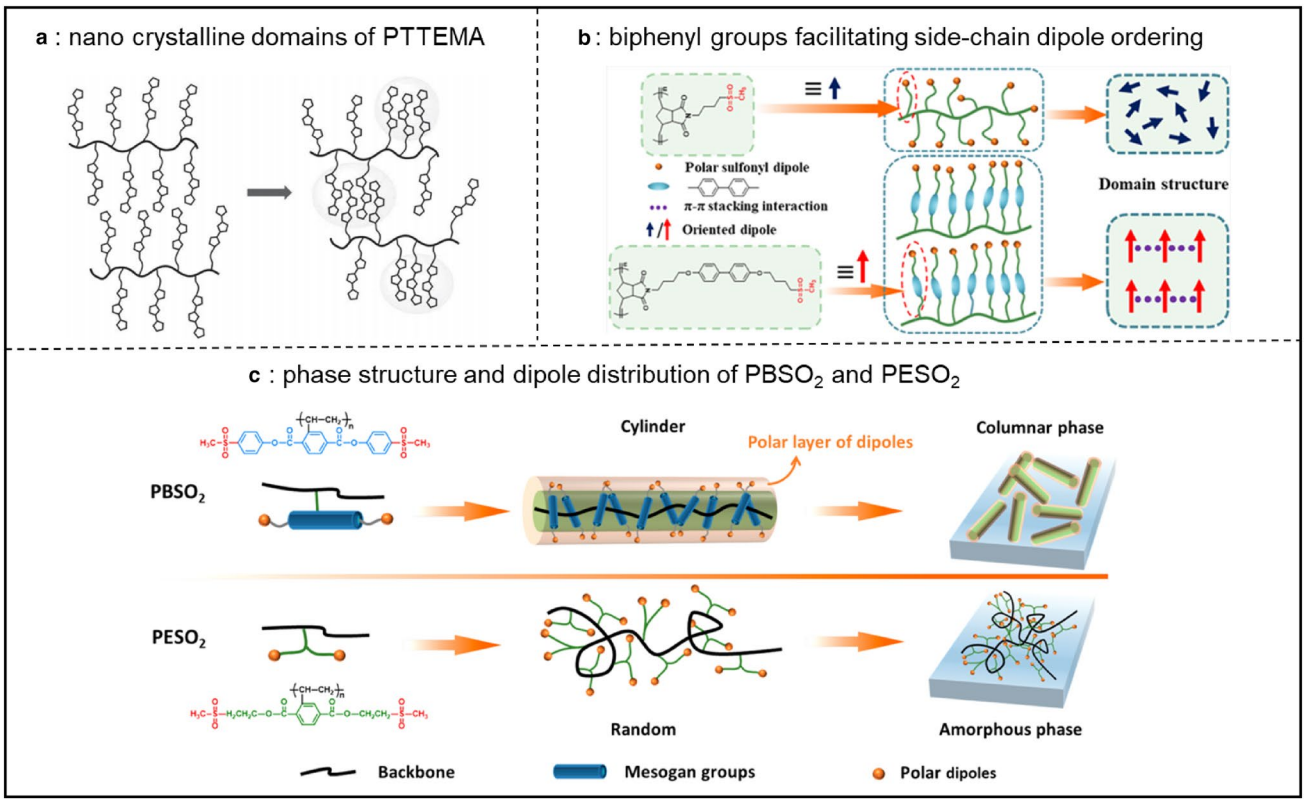

Figure 4. (a) Chemical structure of terthiophene-containing polymer PTTEMA, and its self-organized nano-crystalline domains.[41] Copyright 2013 WILEY–VCH Verlag GmbH & Co. KGaA, Weinheim. (b) Schematic illustration of side-chain dipole ordering facilitated by π–π stacking of the biphenyl groups.[43] Copyright 2021 American Chemical Society. (c) Schematic diagram of the phase structure and dipole distribution of $PBSO_2$ and $PESO_2$.[44] Copyright 2021 American Chemical Society.

sulfonyl at the chain end, resulting in nano-domains of unidirectionally aligned dipole moments [Fig. 4(b)].[43] Consequently, the dielectric constant of biphenyl-containing PBTMD-SO_2 was substantially higher than that of PTMD-SO_2 (11.1 vs. 8.2, 1 kHz).

A recent study by Chen and coworkers investigated the effects of the liquid crystalline (LC) phase on the dielectric properties of side-chain polymer dielectrics.[44] Despite having a significantly higher T_g than its amorphous counterpart $PESO_2$ (195°C vs. 78°C), the LC polymer $PBSO_2$ with rigid side chains exhibited a higher dielectric constant of 20.8 (25 °C, 1 kHz). The approximately 18% improvement in dielectric constant was attributed to the LC-induced side-chain ordering and interfacial polarization between the LC phase and the amorphous region [Fig. 4(c)]. Due to the higher T_g and β relaxation temperature, which constrain segmental chain movement and space charges migration, $PBSO_2$ also exhibited much lower dielectric loss, especially at high frequencies.

However, the enhancement of dielectric constant by side-chain dipole self-assembly is only marginal to fair, which may not always justify the additional efforts required for molecule synthesis and morphology control.

Long-range side-chain ordering with ladder-like polysilsesquioxanes (LPSQs)

Very recently, In and coworkers discovered that LPSQs can function as high-*k* dielectric materials.[45] GLPSQ [Fig. 5(a)] exhibited a significantly higher dielectric constant than CLPSQ [Fig. 5(b)], with values of 8 and 4 at 100 Hz, respectively. This difference was attributed to the higher dipole moment of glycidyl compared to cyclohexyl epoxy. Unlike typical side-chain polymer dielectrics, which usually experience a decline in dielectric constants toward the higher frequencies,[34,37,39,44] the dielectric constants of both GLPSQ and CLPSQ remained almost constant from 10 to 10^6 Hz [Fig. 5(c), (d)]. This behavior suggests very fast and friction-free dipole reorientation, possibly due to the long-range side-chain ordering enabled by the rigid double-stranded siloxane structure, which impedes Si–O internal rotation compared to a single chain. However, the strong XRD peaks representing periodic interchain distances of 17.48 Å and 14.81 Å for GLPSQ and CLPSQ, respectively, disappeared, after UV curing, indicating randomly orientated crosslinking sites [Fig. 5(a), (b)]. Nonetheless, the dielectric constants of UV-cured GLPSQ and CLPSQ increased, likely due to the high-polar hydroxy groups. It should be noted that, in comparison to GLPSQ, which only showed a marginal increase

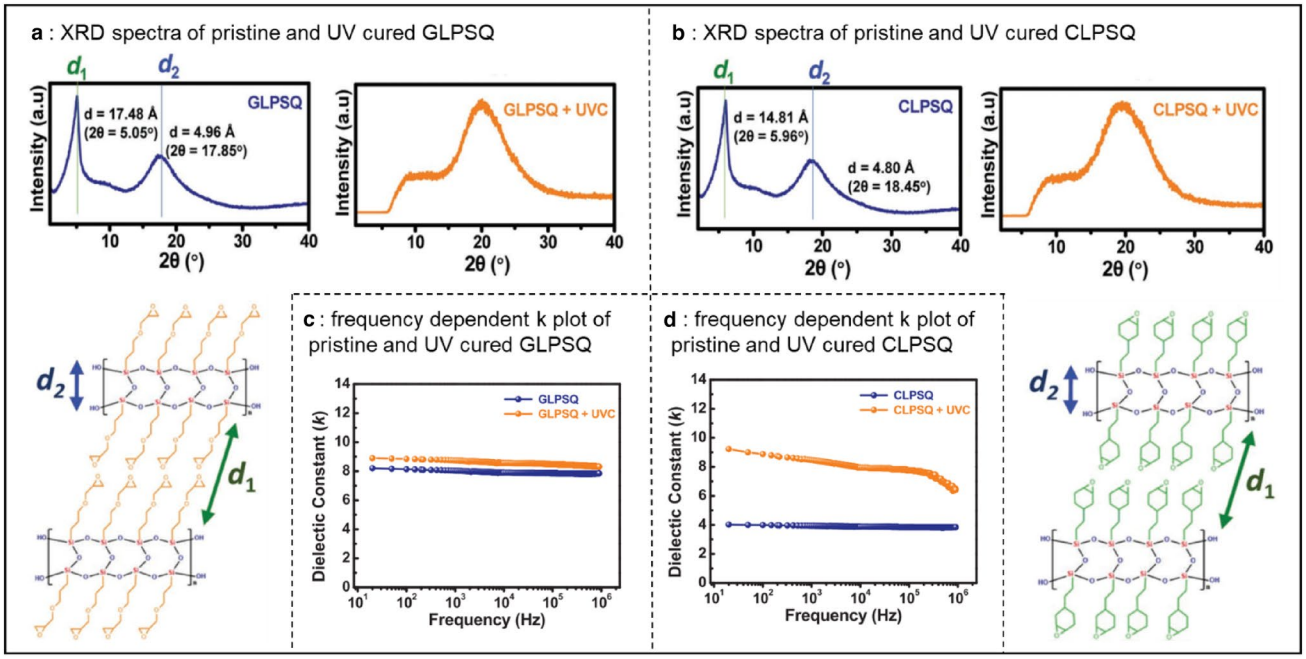

Figure 5. XRD[45] spectra of pristine and UV-cured (a) GLPSQ and (b) CLPSQ. (c) Frequency-dependent *k* plots of pristine and UV-cured GLPSQ. (d) Frequency-dependent *k* plots of pristine and UV-cured CLPSQ. Copyright 2023 Wiley VCH GmbH

in dielectric constant after UV curing, the dielectric constant of UV-cured CLPSQ was significantly higher than its pristine counterpart (~9 vs. 4, 100 Hz). However, it is highly dependent on the frequency, showing a clear declining trend toward higher frequencies. The author ascribed the phenomenon to much higher hydroxyl density and stronger molecular interactions/steric hindrance of UV-cured CLPSQ.

Polysilsesquioxanes (PSQs)[46] have been increasingly explored as dielectric materials for OFETs in recent years.[47–51] However, amorphous PSQs exhibit drawbacks such as severe dielectric loss, high leakage currents, and a high density of charge traps, mainly due to the big number of uncondensed silanol groups. Furthermore, their irregular network structures result in poor morphology control and lack of flexibility. In contrast, LPSQs with double-stranded Si–O–Si backbones significantly reduced uncondensed silanol (Si–OH) groups, which are located entirely at the chain ends.[52] This desired feature makes LPSQs a promising dielectric material with excellent mechanical/optical,[53,54] thermal,[55] and dielectric properties.[56,57] Additionally, the synthesis and functionalization of LPSQs are relatively straightforward.[58] We anticipate the application of LPSQs as high-performance gate dielectric materials for OTFT will become a hot topic in the following years.

Enhancing side-chain dipole mobility by 'rigid free volume'

Thermoplastic polymers

Very recently, polymers of intrinsic microporosity (PIMs)[59,60] were investigated as polymer dielectrics by Zhu and coworkers. They synthesized a rigid and temperature-resistant sulfonylated PIM (SO_2-PIM) with a high dielectric constant up to 6 and a loss as low as 0.005.[61] The outstanding dielectric performance was mainly attributed to the friction-free rotation of the sulfonyl dipoles in the intrinsic nanopores, which is a direct result of the rigid and contorted polymer backbone [Fig. 6(a)]. The same concept was also demonstrated by Yang and coworkers with polyimides of rigid-twisted backbone and flexible-sulfonylated side chains [STP-PI, Fig. 6(b)].[62,63] Comparing to temperature-resistant polymers with more linear and/or flexible backbones,[64,65] STP-PI exhibited higher dielectric constants (5.5–6.5, 100 Hz) with relatively low dielectric loss (0.009–0.011, 100 Hz), despite lower dipole density.

These two examples demonstrate the effectiveness of the 'rigid free volume' approach in achieving low dielectric loss across a broad temperature range. On one hand, the highly rigid polymer structures result in very high T_g, which contribute to low leakage current, high breakdown strength, and low dielectric loss at high temperatures. On the other hand, the rigid and relatively large nanopores isolate dipoles from each other, eliminating dipole–dipole interactions that typically lead to reduced dielectric constant and higher dielectric loss. However, the drawbacks of the thermoplastic approach are also evident. First, thermoplastic polymers featuring 'rigid free volume' are not easily accessible. Significant efforts in organic and polymer synthesis are required to make the desired molecules. Additionally, despite the enhanced dipole mobility, the relatively low dipole density prevents such polymers from achieving a higher dielectric constant.

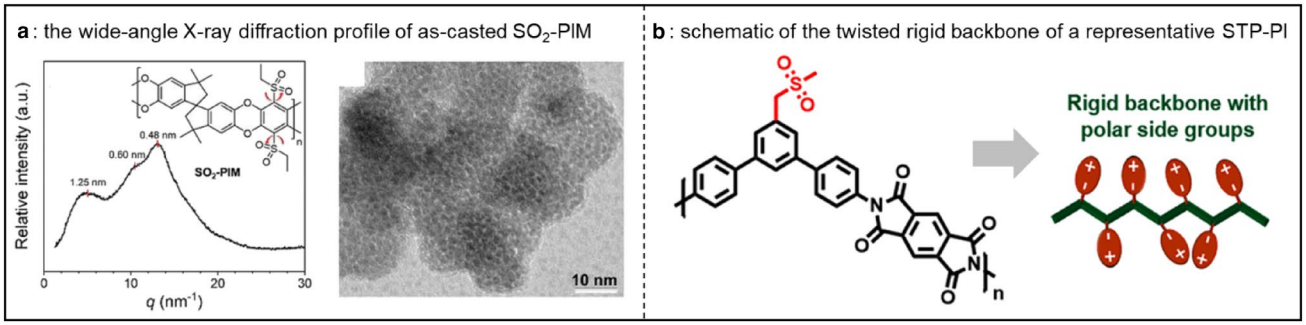

Figure 6. (a) The one-dimensional wide-angle X-ray diffraction profile for the as-cast SO_2-PIM corresponds to different pore sizes from 0.5 to 1.25 nm. The chemical structure of SO_2-PIM is shown as the inset.[61] Copyright 2020 The Royal Society of Chemistry. (b) The chemical structure of a representative STP-PI, and the schematic representing twisted rigid backbone and flexible side-chain dipoles.[63] Copyright 2022 Elsevier B.V.

Thermosets

Alternatively, thermosets can also be utilized to create 'rigid free volume'. In our recent study, a cured star-type thermoset ESPOSS [weight ratio of EP-POSS and EP-Sulfone = 1:1, 3 wt% photo-acid generator PAG 290, and 3 wt% photo-sensitizer ITX, Fig. 7(a)] exhibits a dielectric constant as high as 30 at 1 kHz.[66] In contrast to CLPSQ,[45] ESPOSS exhibited an almost constant dielectric constant from 10 to 1000 Hz, indicating friction-free dipole reorientation. We attribute the superior dielectric constant stability of ESPOSS versus CLPSQ mainly to morphology difference. In UV-cured CLPSQ, the cyclohexyl groups impeded dipole (hydroxyl) reorientation due to steric hindrance.[45] In contrast, reorientations of sulfonyl and hydroxyl in ESPOSS are much less hindered due to the higher fraction of 'rigid free volume' created by the star-type hybrids containing POSS as crosslinking sites[67–71] and rigid polycyclohexyl as linkers [Fig. 7(b)]. It should be noted that our current results are only preliminary. We are currently optimizing formulations and processing conditions, as well as conducting further tests, such as dielectric loss.

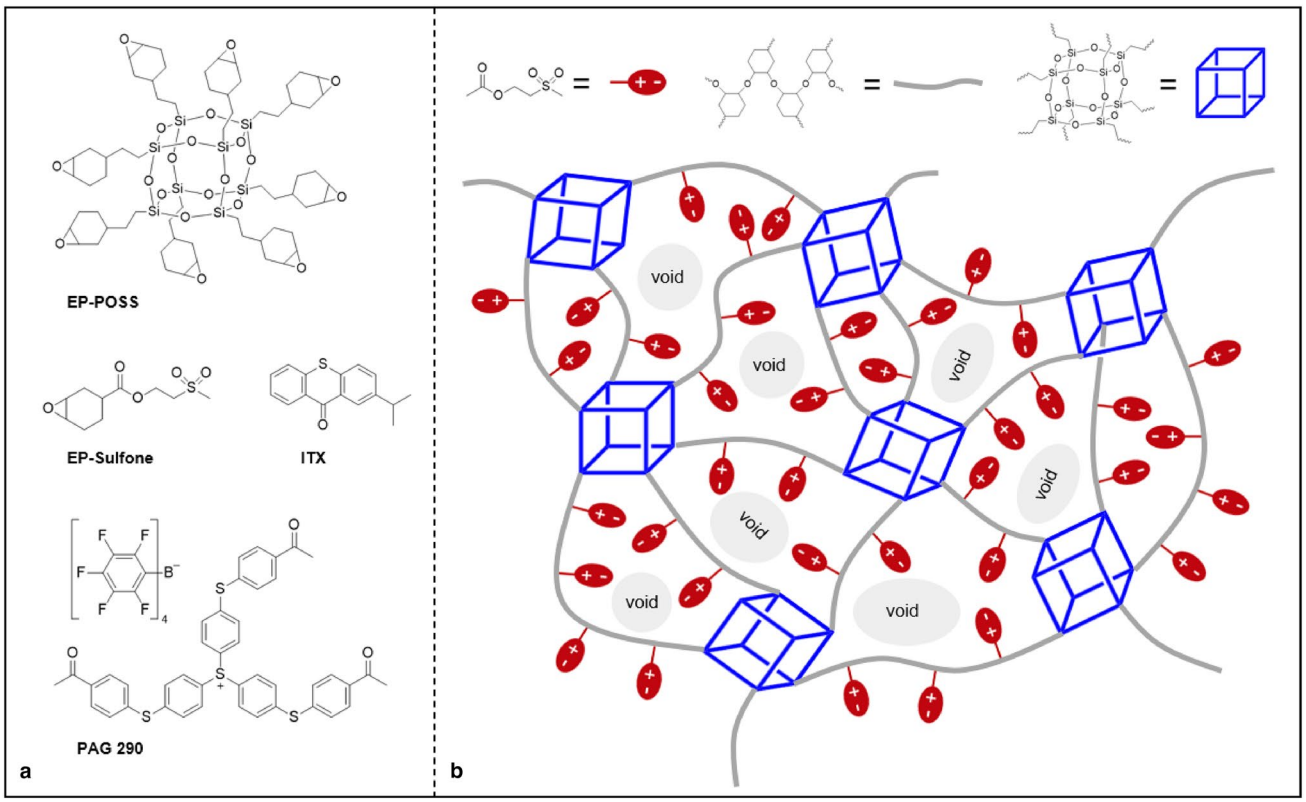

Figure 7. (a) Chemical structures of EP-POSS, EP-Sulfone, ITX, and PAG 290. (b) Schematics of crosslinked network of EP-POSS/EP-Sulfone containing highly mobile side-chain sulfonyl groups.

The advantages of the thermosets approach over that of thermoplastic polymer are as follows: (1) Higher dielectric constant because of higher fractions of free volume and higher dipole density; (2) Significantly reduced material cost due to much less synthetic effort; (3) Much greater material design freedom through formulation adjustment rather than synthesizing new oligomers/polymers.

Creating nanoscale phase separation by block copolymers

Block copolymers are well known for their ability to fabricate nanostructures of various morphologies via self-assembly.[72,73] However, they had not been utilized to enhance dielectric constant until very recently, when Xie and coworkers explored a series of polynorbornene (PNBE)-based block copolymers as high-performance polymer dielectrics.[74–80] In 2020, they reported on block copolymers consisting of high-polar-insulating PNBE blocks and conducting polyacetylene (PA) blocks [Fig. 8(a)], which exhibited a very stable dielectric constant up to 25 across a wide frequency range from 1 kHz to 1 MHz, as well as very low loss at 0.004–0.0015.[79] The block copolymers with well-defined nanostructures also demonstrated linear polarization behavior and low hysteresis, a clear indication of low-level energy dissipation. However, as the length of the conducting PA block increased, the hysteresis loop of the copolymer became large due to increased leakage current. The same group also investigated more sophisticated block copolymers with double-stranded backbones. For example, one of the copolymers containing an ionically conductive block and an insulating block **PBNPF**-(*b*-**PTNP**)$_2$ [Fig. 8(b)] was reported to exhibit outstanding dielectric constant and low loss at 25 and 0.02, respectively.[75] Xie and coworkers further designed a tetra-block copolymer **PBNPF**-*b*-**PBHPF**-(*b*-**PTNP**)$_2$ [Fig. 8(c)] containing an additional conjugated block **PBHPF** with an enhanced dielectric constant as high as 28–33 and low loss at 0.055–0.02 across 10^2–10^6 Hz.[78]

The block copolymer strategy effectively combines dipolar, electronic, and interfacial polarizations, and successfully confine ionic movement within the nanoscale conductive domains. It is noteworthy that block copolymers differ from organic/inorganic composite dielectrics, which rely on the high permittivity of inorganic nanoparticles to boost the dielectric constant. Instead, they are one-component materials characterized by smoother and more homogeneous organic–organic interfaces. Consequently, challenges typically associated with composite dielectrics, such as nanoparticle agglomeration, high dielectric loss, and premature electric breakdown, are no longer prevalent. However, the high cost of block copolymers associated with both monomer and polymer synthesis may pose the biggest hurdle for their industrial applications.

Summary and outlook

As reviewed in Sects. "Traditional high-polar polymer dielectrics" and "New strategies," in addition to conventional main-chain and side-chain high-polar polymers, several novel strategies for constructing high-*k* polymer dielectrics have emerged in recent years. Table I summarizes the key references reviewed in this perspective. From a structure–property standpoint, we would like to propose four principles for designing high-*k* polymer dielectrics.

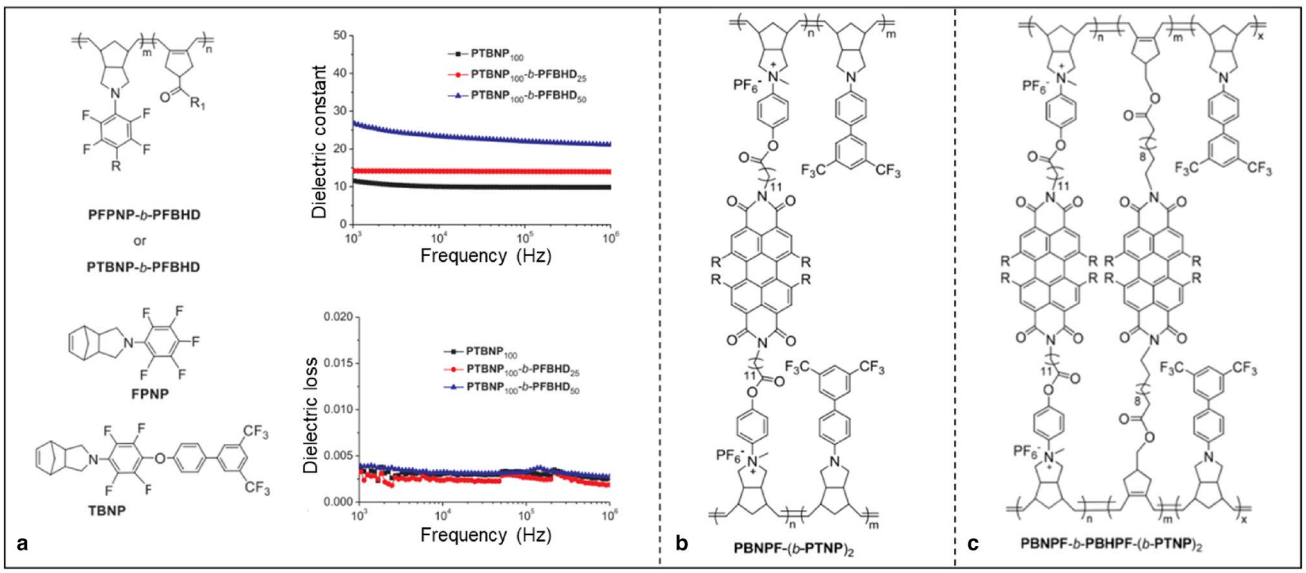

Figure 8. (a) Molecular structure of PNBE-PA block copolymers **PFPNP**-*b*-**PFBHD** and **PTBNP**-*b*-**PFBHD**, and their frequency-dependent dielectric constant and dielectric loss plots.[79] Copyright 2019 Elsevier Ltd. (b) Molecular structure of double-stranded block copolymer **PBNPF**-(*b*-**PTNP**)$_2$.[75] Copyright 2017 Elsevier Ltd. (c) Molecular structure of double-stranded block copolymer **PBNPF**-*b*-**PBHPF**-(*b*-**PTNP**)$_2$.[78] Copyright 2018 American Chemical Society.

Table I. Summary of the key references reviewed in this perspective.

Entries	Strategy	Dielectric constant/1 kHz	Dielectric loss/1 kHz	Dielectric constant enhancing mechanism	References
1	Main chain	5.23	0.00324	a, c	[24]
2		8.6	~0.1	a	[26]
3		9	~0.3	a	[27]
4	Side chain	10.5	0.02	c	[31]
5		8.2	0.003	b, c	[32]
6		7.7–9.1	0.003–0.02	b, c	[35]
7	Side-chain dipole ordering	~11	~0.02	d–f	[41]
8		11.1	0.075	d	[43]
9		20.8	0.02	d, e	[44]
10		~9	n.a	a	[45]
11	Rigid free volume	6	0.005	a	[61]
12*		5.5–6.5	~0.01	a	[62,63]
13		30	n.a	a, c	[66]
14	Nanoscale phase separation	25	0.02	c, e, g	[75]
15		~30	~0.06	c, e, f, g	[78]
16		25	~0.003	c, e, f	[79]

*Dielectric constant and loss were measured at 100 Hz; a dipole mobility, b dipole density, c dipole moment, d dipole ordering, e interfacial orientation, f electronic orientation, g ionic orientation.

First, we would like to re-emphasize that side-chain dipole is preferred over main-chain dipole to achieve high dielectric constant, while it is possible for main-chain high-polar polymers to achieve high k by enhancing dipole mobility; in most cases, it is accompanied by high dielectric loss (see Table I, Entries 2 and 3), because high dipole mobility results in low T_g and high spacious charge mobility, both contributing to high dielectric loss. In contrast, the reorientation of side-chain dipoles is based on β- and γ-relaxation, which do not involve segmental movement of the main chain (α-transition). As a result, high k and low loss can be achieved simultaneously (see Table I, Entries 4–6).

Second, 'rigid free volume,' which significantly improves side-chain dipole mobility while effectively suppressing main-chain mobility, is highly desirable for achieving high dielectric constant and low loss. In general, 'rigid free volume' can be realized through either molecular or morphological strategies. For example, in the case of PIMs, the 'rigid free volume' is primarily a direct result of specific molecular structures (see Table I, Entries 11 and 12). In contrast, the free volume of rigid POSS networks is largely ascribed to its star-shape morphology and rigid linkers (see Table I, Entry 13).

Third, self-assembly-facilitated nanoscale phase separation can be exploited to induce interfacial, ionic, and electric polarizations in one-component polymer dielectrics. As shown in Table I, interfacial and ionic polarizations play crucial roles in achieving remarkably high dielectric constants for block copolymers (see Table I, Entries 14–16). Smooth and defect-free interfaces between distinct organic phases are desirable for expediting polarization and mitigating charge traps. Furthermore, the sea-island morphology of the block copolymers, characterized by conductive polymer segments as the island phase and insulating segments as the sea phase, efficiently confines electric and/or ionic conduction within the conductive domains. Consequently, polymer dielectrics with self-assembly-induced nanoscale phase separation surpass conventional composite dielectrics[16,81,82] and polymer electrolytes,[83] offering remarkably lower losses and vastly improved insulating properties.

Finally, thermosets are preferred over high-molecular-weight thermoplastic polymers for polymer gate dielectrics used in OFETs. The advantages of curable thermosets are as follows: (1) Thermosets are much readily soluble in commonly used organic solvents, facilitating straightforward thin-film fabrication through various solution-based coating techniques. In contrast, many thermoplastic polymers can only be processed by melting and thermoforming, which is not compatible with OFET manufacturing. (2) Depending on crosslinking degree, the T_g of cured thermosets can be dramatically increased comparing to the pristine monomers/oligomers, providing similarly low loss compared to thermoplastic polymers. (3) Thanks to the vastly readily available raw materials, particularly acrylate and epoxy monomers/oligomers, thermosets offer much greater material design freedom without the heavy synthetic efforts normally required by thermoplastic polymers.

In the context of fabricating industrial-scale organic circuits and achieving product miniaturization, we are convinced that UV-patternable polymer gate dielectrics[84–87] are highly advantageous, as they enable densely integrated organic circuits in a scalable and economic manner.[88–90] Very recently, perfluorophenyl azides (PFAs)[89] and organic bis-diazirine[88] have emerged as powerful universal UV crosslinkers. Without the addition of any initiator or sensitizer, they readily react with

plain alkyl chains via active nitrene[91] or carbene[92] species under UV exposure. However, we will not delve into further details on this topic as it is beyond the scope of this perspective.

Looking forward, we anticipate the recent progress in high-*k* polymer dielectrics will significantly improve the performance of OFET devices. For example, OFETs utilizing STP-PI [Fig. 6(b)] as the gate dielectric layer demonstrated a substantially lower operating voltage of 5 V compared to 15 V for non-grafted PI.[63] In addition, the charge mobility and on/off ratio increased from 0.75 $cm^2\ V^{-1}\ s^{-1}$ and 4.5×10^4 to 4.03 $cm^2\ V^{-1}\ s^{-1}$ and 1×10^5, respectively. It will be intriguing to observe the extent of improvement in OFET performance with utilization of other polymer dielectrics, particularly those with extremely high dielectric constants such as ESPOSS and block polymers, as gate dielectrics. This advancement may represent a significant step forward in achieving high-performance, low-power-consumption, and affordable OFETs for everyday applications in the foreseeable future.

Acknowledgments

This work was funded by Organic and Biotechnology Department, Global Research, Corning Incorporated.

Author contributions

Y. Li conceived the presented idea, drafted, and modified the manuscript. M. He helped to modify the manuscript structure with his professional background.

Data availability

Not applicable.

Declarations

Conflict of interest

The authors declare no conflict of interest.

References

1. A. Tsumura, H. Koezuka, T. Ando, Macromolecular electronic device: field-effect transistor with a polythiophene thin film. Appl. Phys. Lett. **49**(18), 1210–1212 (1986)
2. M. Sommer, Development of conjugated polymers for organic flexible electronics. In *Organic Flexible Electronics: Fundamentals, Devices, and Applications* (Elsevier, Amsterdam, 2020), pp. 27–70
3. L. Li, L. Han, H. Hu, R. Zhang, A review on polymers and their composites for flexible electronics. Mater. Adv. **4**(3), 726–746 (2022)
4. H. Liu, D. Liu, J. Yang, H. Gao, Y. Wu, Flexible electronics based on organic semiconductors: from patterned assembly to integrated applications. Small **19**(11), 2206938 (2023)
5. Z. Shen, W. Huang, L. Li, H. Li, J. Huang, J. Cheng, Y. Fu, Research progress of organic field-effect transistor based chemical sensors. Small **19**(41), 2302406 (2023)
6. J.C. Yang, J. Mun, S.Y. Kwon, S. Park, Z. Bao, S. Park, Electronic Skin: recent progress and future prospects for skin-attachable devices for health monitoring, robotics, and prosthetics. Adv. Mater. **31**(48), 1904765 (2019)
7. Z. Ma, D. Kong, L. Pan, Z. Bao, Skin-inspired electronics: emerging semiconductor devices and systems. J. Semicond. **41**(4), 041601 (2020)
8. M.R. Cavallari, L.M. Pastrana, C.D.F. Sosa, A.M.R. Marquina, J.E.E. Izquierdo, F.J. Fonseca, C.A. de Amorim, L.G. Paterno, I. Kymissis, Organic thin-film transistors as gas sensors: a review. Materials **14**(1), 1–32 (2021)
9. S. Zhang, Y. Zhao, X. Du, Y. Chu, S. Zhang, J. Huang, Gas sensors based on nano/microstructured organic field-effect transistors. Small **15**(12), 1805196 (2019)
10. C. Zhang, P. Chen, W. Hu, Organic field-effect transistor-based gas sensors. Chem. Soc. Rev. **44**(8), 2087–2107 (2015)
11. M.J. Chan, Y.J. Li, C.C. Wu, Y.C. Lee, H.W. Zan, H.F. Meng, M.H. Hsieh, C.S. Lai, Y.C. Tian, Breath ammonia is a useful biomarker predicting kidney function in chronic kidney disease patients. Biomedicines **8**(11), 468 (2020)
12. W.L. Chang, C.C. Chang, Y.T. Lee, A.D. Tran Thi, C.C. Chen, H.F. Meng, H.W. Zan, C.J. Lu, M. He, Y. Li, Gas emission from human skin positions detected by vertical-channel organic semiconductor sensor. Sens. Actuators B **343**, 129994 (2021)
13. Y. Duan, B. Zhang, S. Zou, C. Fang, Q. Wang, Y. Shi, Y. Li, Low-power-consumption organic field-effect transistors. J. Phys. Mater. **3**(1), 014009 (2020)
14. J. Qiu, Q. Gu, Y. Sha, Y. Huang, M. Zhang, Z. Luo, Preparation and application of dielectric polymers with high permittivity and low energy loss: a mini review. J. Appl. Polym. Sci. **139**(24), 52367 (2022)
15. S. Wang, C. Yang, X. Li, H. Jia, S. Liu, X. Liu, T. Minari, Q. Sun, Polymer-based dielectrics with high permittivity and low dielectric loss for flexible electronics. J. Mater. Chem. C **10**(16), 6196–6221 (2022)
16. R.P. Ortiz, A. Facchetti, T.J. Marks, High-k organic, inorganic, and hybrid dielectrics for low-voltage organic field-effect transistors. Chem. Rev. **110**(1), 205–239 (2010)
17. B. Wang, W. Huang, L. Chi, M. Al-Hashimi, T.J. Marks, A. Facchetti, High-k gate dielectrics for emerging flexible and stretchable electronics. Chem. Rev. **118**(11), 5690–5754 (2018)
18. Y. Wang, X. Huang, T. Li, L. Li, X. Guo, P. Jiang, Polymer-based gate dielectrics for organic field-effect transistors. Chem. Mater. **31**(7), 2212–2240 (2019)
19. A. Liu, H. Zhu, H. Sun, Y. Xu, Y.Y. Noh, Solution processed metal oxide high-κ dielectrics for emerging transistors and circuits. Adv. Mater. **30**(33), 1706364 (2018)
20. S. Park, C.H. Kim, W.J. Lee, S. Sung, M.H. Yoon, Sol–gel metal oxide dielectrics for all-solution-processed electronics. Mater. Sci. Eng. R **114**, 1–22 (2017)
21. B.M. Pirzada, S. Sabir, Polymer-based nanocomposites for significantly enhanced dielectric properties and energy storage capability. In *Polymer-Based Nanocomposites for Energy and Environmental Applications: A Volume in Woodhead Publishing Series in Composites Science and Engineering* (Woodhead Publishing, Sawston, 2018), pp. 132–183
22. Y. Zhou, S.T. Han, V.A.L. Roy, Nanocomposite dielectric materials for organic flexible electronics. In *Nanocrystalline Materials: Their Synthesis–Structure–Property Relationships and Applications* (Elsevier, Amsterdam, 2013), pp. 195–220
23. L. Zhu, Exploring strategies for high dielectric constant and low loss polymer dielectrics. J. Phys. Chem. Lett. **5**(21), 3677–3687 (2014)
24. H. Tong, A. Ahmad, J. Fu, H. Xu, T. Fan, Y. Hou, J. Xu, Revealing the correlation between molecular structure and dielectric properties of carbonyl-containing polyimide dielectrics. J. Appl. Polym. Sci. **136**(34), 47883 (2019)
25. D. Wu, X. Zhao, X. Li, J. Dong, Q. Zhang, Polyimide film containing sulfone groups with high dielectric properties. Polymer **256**, 125221 (2022)
26. Y. Feng, L. Yang, G. Qu, T. Suga, H. Nishide, G. Chen, S. Li, Optimizing the interdomain spacing in alicyclic polythiourea toward high-energy-storable dielectric material. Macromol. Rapid Commun. **41**(13), 2000167 (2020)
27. J. Lv, L. Huang, J. Ning, C. Tian, Q. Liu, F. Zeng, W. Kong, X. Cai, A high dielectric constant copolyamide based on high dipole density. J. Polym. Res. **29**(3), 106 (2022)
28. Y. Thakur, B. Zhang, R. Dong, W. Lu, C. Iacob, J. Runt, J. Bernholc, Q.M. Zhang, Generating high dielectric constant blends from lower dielectric constant dipolar polymers using nanostructure engineering. Nano Energy **32**, 73–79 (2017)
29. J.W. Zha, Y. Tian, M.S. Zheng, B. Wan, X. Yang, G. Chen, High-temperature energy storage polyimide dielectric materials: polymer multiple-structure design. Mater. Today Energy **31**, 101217 (2023)

30. H. Tong, J. Fu, A. Ahmad, T. Fan, Y. Hou, J. Xu, Sulfonyl-containing polyimide dielectrics with advanced heat resistance and dielectric properties for high-temperature capacitor applications. Macromol. Mater. Eng. **304**(4), 1800709 (2019)
31. J. Wei, Z. Zhang, J.K. Tseng, I. Treufeld, X. Liu, M.H. Litt, L. Zhu, Achieving high dielectric constant and low loss property in a dipolar glass polymer containing strongly dipolar and small-sized sulfone groups. ACS Appl. Mater. Interfaces **7**(9), 5248–5257 (2015)
32. Z. Zhang, D.H. Wang, M.H. Litt, L.S. Tan, L. Zhu, High-temperature and high-energy-density dipolar glass polymers based on sulfonylated poly(2, 6-dimethyl-1, 4-phenylene oxide). Angew. Chem. Int. Ed. **57**(6), 1528–1531 (2018)
33. J. Wei, T. Ju, W. Huang, J. Song, N. Yan, F. Wang, A. Shen, Z. Li, L. Zhu, High dielectric constant dipolar glass polymer based on sulfonylated poly(ether ether ketone). Polymer **178**, 121688 (2019)
34. Y. Tang, H. Yao, W. Xu, L. Zhu, Y. Zhang, Z. Jiang, Side-chain-type high dielectric-constant dipolar polyimides with temperature resistance. Macromol. Rapid Commun. **44**(2), 2200639 (2023)
35. Y.F. Zhu, Z. Zhang, M.H. Litt, L. Zhu, High dielectric constant sulfonyl-containing dipolar glass polymers with enhanced orientational polarization. Macromolecules **51**(16), 6257–6266 (2018)
36. R. Matsuno, Y. Takagaki, T. Ito, H. Yoshikawa, S. Takamatsu, A. Takahara, Highly dielectric rubber bearing cyanoethyl group with various side-chain structures. Macromolecules **53**(22), 10128–10136 (2020)
37. T. Xu, Y. Liu, Y. Bu, S. Shu, S. Fan, M. Cao, T. Liu, J. Zou, J. Su, Newly synthesized high-k polymeric dielectrics with cyclic carbonate functionality for highly stability organic field-effect transistor applications. Adv. Electron. Mater. **9**(1), 2200984 (2023)
38. H.J. Kwon, H. Ye, K. Shim, H.G. Girma, X. Tang, B. Lim, Y. Kim, J. Lee, C.E. Park, S.H. Jung, J.M. Park, Y.J. Jung, D.H. Hwang, H. Kong, S.H. Kim, Newly synthesized nonvacuum processed high-k polymeric dielectrics with carboxyl functionality for highly stable operating printed transistor applications. Adv. Funct. Mater. **31**(5), 2007304 (2021)
39. J. Xie, H. Liu, J. Hu, X. Zhao, S. Song, S. Sun, M. Zhang, Solution-processed linear methyl methacrylate-*co*-glycidyl methacrylate films with excellent dielectric and energy storage characters. Mater. Adv. **3**, 6619–6627 (2022)
40. C. Liu, S. Liu, J. Lin, L. Wang, Y. Huang, X. Liu, Component adjustment of poly(arylene ether nitrile) with sulfonic and carboxylic groups for dielectric films. Polymers **11**(7), 1135 (2019)
41. Y. Qiao, M.S. Islam, K. Han, E. Leonhardt, J. Zhang, Q. Wang, H.J. Ploehn, C. Tang, Polymers containing highly polarizable conjugated side chains as high-performance all-organic nanodielectric materials. Adv. Funct. Mater. **23**(45), 5638–5646 (2013)
42. X. Yin, Y. Qiao, M.R. Gadinski, Q. Wang, C. Tang, Flexible thiophene polymers: a concerted macromolecular architecture for dielectrics. Polym. Chem. **7**(17), 2929–2933 (2016)
43. H. Xu, G. He, S. Chen, S. Chen, R. Qiao, H. Luo, D. Zhang, All-organic polymer dielectrics containing sulfonyl dipolar groups and π–π stacking interaction in side-chain architectures. Macromolecules **54**(17), 8195–8206 (2021)
44. H. Xu, S. Chen, S. Chen, R. Qiao, H. Li, H. Luo, D. Zhang, Constructing high-performance dielectrics via molecular and phase engineering in dipolar polymers. ACS Appl. Energy Mater. **4**(3), 2451–2462 (2021)
45. H. Ye, E. Park, S.C. Shin, G. Murali, D. Kim, J. Lee, I.H. Kim, S.J. Kim, S.H. Kim, Y.J. Jeong, I. In, Photopatternable high-k polysilsesquioxane dielectrics for organic integrated devices: effects of UV curing on chemical and electrical properties. Adv. Funct. Mater. **33**(19), 2214865 (2023)
46. R.H. Baney, M. Itoh, A. Sakakibara, T. Suzuki, Silsesquioxanes. Chem. Rev. **95**(5), 1409–1430 (1995)
47. Y. Kim, J. Roh, J.H. Kim, C.M. Kang, I.N. Kang, B.J. Jung, C. Lee, D.H. Hwang, Photocurable propyl-cinnamate-functionalized polyhedral oligomeric silsesquioxane as a gate dielectric for organic thin film transistors. Org. Electron. **14**(9), 2315–2323 (2013)
48. Y. Matsuda, Y. Nakahara, D. Michiura, K. Uno, I. Tanaka, High-mobility 6, 13-bis(triisopropylsilylethynyl) pentacene transistors using solution-processed polysilsesquioxane gate dielectric layers. J. Nanosci. Nanotechnol. **16**(4), 3273–3276 (2016)
49. Y. Nakahara, H. Kawa, J. Yoshiki, M. Kumei, H. Yamamoto, F. Oi, H. Yamakado, H. Fukuda, K. Kimura, Ultra-thin films of polysilsesquioxanes possessing 3-methacryloxypropyl groups as gate insulator for organic field-effect transistors. Thin Solid Films **520**(24), 7195–7199 (2012)
50. S. Okada, Y. Nakahara, K. Uno, I. Tanaka, Ester-free cross-linker molecules for ultraviolet-light-cured polysilsesquioxane gate dielectric layers of organic thin-film transistors. Jpn. J. Appl. Phys. **57**(4), 040313 (2018)
51. H. Shibao, Y. Nakahara, K. Uno, I. Tanaka, Investigation of ultraviolet light curable polysilsesquioxane gate dielectric layers for pentacene thin film transistors. J. Nanosci. Nanotechnol. **16**(4), 3327–3331 (2016)
52. S.S. Choi, A.S. Lee, S.S. Hwang, K.Y. Baek, Structural control of fully condensed polysilsesquioxanes: ladderlike vs cage structured polyphenylsilsesquioxanes. Macromolecules **48**(17), 6063–6070 (2015)
53. J.T. Leem, W.C. Seok, J.B. Yoo, S. Lee, H.J. Song, Hard coating materials based on photo-reactive silsesquioxane for flexible application: improvement of flexible and hardness properties by high molecular weight. Polymers **13**(10), 1564 (2021)
54. H. Lee, Y. Lee, S.W. Lee, S.M. Kang, Y.H. Kim, W. Jo, T.S. Kim, J. Jang, B.S. Bae, Elongation improvement of transparent and flexible surface protective coating using polydimethylsiloxane-anchored epoxy-functionalized siloxane hybrid composite for reliable out-foldable displays. Composites B **225**, 109313 (2021)
55. G. Choe, J. Kim, S.C. Shin, Y.R. Jeong, S.J. Kim, B.S. Choi, S. Nam, P. Paoprasert, N. Thongsai, E. Park, B. Kang, G. Murali, S.J. Kim, I. In, T.K. An, Y.J. Jeong, High-k and high-temperature-resistant polysilsesquioxane: potential for solution-processed metal oxide semiconductor transistors operating at low voltage. Mater. Today Commun. (2023). https://doi.org/10.1016/j.mtcomm.2023.105331
56. M. Pei, A.S. Lee, S.S. Hwang, H. Yang, Ladder-like polysilsesquioxane dielectrics for organic field-effect transistor applications. J. Mater. Chem. C **5**(42), 10955–10964 (2017)
57. H. Ye, H.J. Kwon, S.C. Shin, H.Y. Lee, Y.H. Park, X. Tang, R. Wang, K. Lee, J. Hong, Z. Li, W. Jeong, J. Kim, C.E. Park, J. Lee, T.K. An, I. In, S.H. Kim, The hidden potential of polysilsesquioxane for high-k: analysis of the origin of its dielectric nature and practical low-voltage-operating applications beyond the unit device. Adv. Funct. Mater. **32**(7), 2104030 (2022)
58. Y.H. Kim, G.M. Choi, J.G. Bae, Y.H. Kim, B.S. Bae, High-performance and simply-synthesized ladder-like structured methacrylate siloxane hybrid material for flexible hard coating. Polymers **10**(4), 449 (2018)
59. N.B. McKeown, The synthesis of polymers of intrinsic microporosity (PIMs). Sci. China Chem. **60**(8), 1023–1032 (2017)
60. Y. Wang, X. Ma, B.S. Ghanem, F. Alghunaimi, I. Pinnau, Y. Han, Polymers of intrinsic microporosity for energy-intensive membrane-based gas separations. Mater. Today Nano **3**, 69–95 (2018)
61. Z. Zhang, J. Zheng, K. Premasiri, M.-H. Kwok, Q. Li, R. Li, S. Zhang, M.H. Litt, X.P.A. Gao, L. Zhu, High-κ polymers of intrinsic microporosity: a new class of high temperature and low loss dielectrics for printed electronics. Mater. Horiz. **7**(2), 592–597 (2020)
62. W. Zheng, Z. Li, K. Chen, S. Liu, Z. Chi, J. Xu, Y. Zhang, Temperature-resistant intrinsic high dielectric constant polyimides: more flexibility of the dipoles, larger permittivity of the materials. Molecules **27**(19), 6337 (2022)
63. W. Zheng, T. Yang, L. Qu, X. Liang, C. Liu, C. Qian, T. Zhu, Z. Zhou, C. Liu, S. Liu, Z. Chi, J. Xu, Y. Zhang, Temperature resistant amorphous polyimides with high intrinsic permittivity for electronic applications. Chem. Eng. J. **436**, 135060 (2022)
64. T. Zhu, Q. Yu, W. Zheng, R. Bei, W. Wang, M. Wu, S. Liu, Z. Chi, Y. Zhang, J. Xu, Intrinsic high-k-low-loss dielectric polyimides containing *ortho*-position aromatic nitrile moieties: reconsideration on Clausius-Mossotti equation. Polym. Chem. **12**(16), 2481–2489 (2021)
65. W. Huang, T. Ju, R. Li, Y. Duan, Y. Duan, J. Wei, L. Zhu, High-κ and high-temperature dipolar glass polymers based on sulfonylated and cyanolated poly(arylene ether)s for capacitive energy storage. Adv. Electron. Mater. **9**(1), 2200414 (2023)
66. Y. Li, X. Li, M. He, WO2024019905A1 (n.d.)
67. T. Pawlak, A. Kowalewska, B. Zgardzińska, M.J. Potrzebowski, Structure, dynamics, and host–guest interactions in POSS functionalized cross-linked nanoporous hybrid organic–inorganic polymers. J. Phys. Chem. C **119**(47), 26575–26587 (2015)

68. E.T. Kopesky, S.G. Boyes, N. Treat, R.E. Cohen, G.H. McKinley, Thermorheological properties near the glass transition of oligomeric poly(methyl methacrylate) blended with acrylic polyhedral oligomeric silsesquioxane nanocages. Rheol. Acta **45**(6), 971–981 (2006)
69. Y. Qin, F. Zhu, M. Luo, L. Zhang, Catalyst-free preparation of polyhedral oligomeric silsesquioxanes containing Organic-Inorganic hybrid mesoporous nanocomposites. J. Appl. Polym. Sci. **121**(1), 97–101 (2011)
70. P. Sangtrirutnugul, T. Chaiprasert, W. Hunsiri, T. Jitjaroendee, P. Songkhum, K. Laohhasurayotin, T. Osotchan, V. Ervithayasuporn, Tunable porosity of cross-linked-polyhedral oligomeric silsesquioxane supports for palladium-catalyzed aerobic alcohol oxidation in water. ACS Appl. Mater. Interfaces **9**(14), 12812–12822 (2017)
71. T. Seçkin, S. Köytepe, H.I. Adigüzel, Molecular design of POSS core star polyimides as a route to low-κ dielectric materials. Mater. Chem. Phys. **112**(3), 1040–1046 (2008)
72. I.W. Hamley, Ordering in thin films of block copolymers: fundamentals to potential applications. Prog. Polym. Sci. **34**(11), 1161–1210 (2009)
73. Y. Lu, J. Lin, L. Wang, L. Zhang, C. Cai, Self-assembly of copolymer micelles: higher-level assembly for constructing hierarchical structure. Chem. Rev. **120**(9), 4111–4140 (2020)
74. W. Liu, X. Liao, Y. Li, Q. Zhao, M. Xie, R. Sun, Nanostructured high-performance dielectric block copolymers. Chem. Commun. **51**(83), 15320–15323 (2015)
75. J. Chen, C. Long, H. Li, H. Han, R. Sun, M. Xie, Double-stranded block copolymer with dual-polarized linker for improving dielectric and electrical energy storage performance. Polymer **127**, 259–268 (2017)
76. W. Liu, J. Chen, D. Zhou, X. Liao, M. Xie, R. Sun, A high-performance dielectric block copolymer with a self-assembled superhelical nanotube morphology. Polym. Chem. **8**(4), 725–734 (2017)
77. J. Chen, R. Sun, X. Liao, H. Han, Y. Li, M. Xie, Tandem metathesis polymerization-induced self-assembly to nanostructured block copolymer and the controlled triazolinedione modification for enhancing dielectric properties. Macromolecules **51**(24), 10202–10213 (2018)
78. J. Chen, Y. Wang, H. Li, H. Han, X. Liao, R. Sun, X. Huang, M. Xie, Rational design and modification of high-k bis(double-stranded) block copolymer for high electrical energy storage capability. Chem. Mater. **30**(3), 1102–1112 (2018)
79. H. Han, D. Zhou, Q. Ren, F. Ma, C. Ma, M. Xie, High-performance all-polymer dielectric and electrical energy storage materials containing conjugated segment and multi-fluorinated pendants. Eur. Polym. J. **122**, 109376 (2020)
80. J. Gong, C. Ma, Y. Quan, R. Sun, X. Liao, H. Peng, M. Xie, Synthesis of dielectric polymers with bipyridyl ligand and metal complex by ring-opening metathesis polymerization. Polymer **231**, 124127 (2021)
81. Y.J. Kim, J. Kim, Y.S. Kim, J.K. Lee, TiO_2–poly(4-vinylphenol) nanocomposite dielectrics for organic thin film transistors. Org. Electron. **14**(12), 3406–3414 (2013)
82. A. Kösemen, High-performance organic field-effect transistors fabricated with high-k composite polymer gel dielectrics. J. Electron. Mater. **48**(12), 7819–7826 (2019)
83. H. Du, X. Lin, Z. Xu, D. Chu, Electric double-layer transistors: a review of recent progress. J. Mater. Sci. **50**(17), 5641–5673 (2015)
84. Q. Shi, Y. Xie, S. Cai, W.Y. Lee, Z. Bao, J.R. Matthews, K.L. Simonton, T.E. Myers, R.A. Bellman, M. He, H.H. Fong, High performance tetrathienoacene-DDP based polymer thin-film transistors using a photo-patternable epoxy gate insulating layer. Org. Electron. **15**(5), 991–996 (2014)
85. S. Yoo, D.G. Kim, H. Park, J. Ha, J. Kim, J.C. Won, Y.H. Kim, Solution-processable and photocurable aromatic polyurea gate dielectrics for high-performance organic thin-film transistors. Mater. Res. Bull. **157**, 112005 (2023)
86. J. Zou, H. Wang, X. Zhang, X. Wang, Z. Shi, Y. Jiang, Z. Cui, D. Yan, Polyimide-based gate dielectrics for high-performance organic thin film transistors. J. Mater. Chem. C **7**(24), 7454–7459 (2019)
87. J.S. Kwon, H.W. Park, D.H. Kim, Y.J. Kwark, Solvent-free processable and photo-patternable hybrid gate dielectric for flexible top-gate organic field-effect transistors. ACS Appl. Mater. Interfaces **9**(6), 5366–5374 (2017)
88. Y.Q. Zheng, Y. Liu, D. Zhong, S. Nikzad, S. Liu, Z. Yu, D. Liu, H.C. Wu, C. Zhu, J. Li, H. Tran, J.B.H. Tok, Z. Bao, Monolithic optical microlithography of high-density elastic circuits. Science **373**(6550), 88–94 (2021)
89. M.J. Kim, M. Lee, H. Min, S. Kim, J. Yang, H. Kweon, W. Lee, D.H. Kim, J.H. Choi, D.Y. Ryu, M.S. Kang, B.S. Kim, J.H. Cho, Universal three-dimensional crosslinker for all-photopatterned electronics. Nat. Commun. **11**(1), 1520 (2020)
90. R. Chen, X. Wang, X. Li, H. Wang, M. He, L. Yang, Q. Guo, S. Zhang, Y. Zhao, Y. Li, L. Yunqi, D. Wei, A comprehensive nano-interpenetrating semiconducting photoresist toward all-photolithography organic electronics. Sci. Adv. **7**(25), eabg0659 (2021)
91. L.H. Liu, M. Yan, Perfluorophenyl azides: new applications in surface functionalization and nanomaterial synthesis. Acc. Chem. Res. **43**(11), 1434–1443 (2010)
92. J. Brunner, H. Senn, F.M. Richards, 3-Trifluoromethyl-3-phenyldiazirine. A new carbene generating group for photolabeling reagents. J. Biol. Chem. **255**(8), 3313–3318 (1980)